Reducing heat loss from solar hot water storage tanks using passive baffles

S.T. Paing, T.N. Anderson* and R.J. Nates

Department of Mechanical Engineering, Auckland University of Technology, New Zealand

Abstract

Solar water heating systems with thermal storage are one of the simplest ways of reducing energy demand for domestic water heating. Over the years, researchers have attempted to improve the thermal performance of storage tanks using various means, including baffle-type devices to control mixing during charging and discharging of the tank. However, one modification that has been overlooked is the use of passive baffles that suppress the natural convection inside the tank with a view to reducing their standing heat loss.

Considering this, this study examined the use of concentric vertically mounted baffles on the natural convection inside a vertical cylindrical storage tank. To this end, a numerical model of a tank with a baffle was developed using computational fluid dynamics (CFD) and validated using experimental data. The results showed that a simple concentrically mounted baffle could reduce the natural convection heat transfer coefficient by up to 40%.

Nomenclature

$\boldsymbol{A_{total}}$	Total surface area ($\boldsymbol{m^2}$)
A	Tank surface area ($\boldsymbol{m^2}$)
AR	Aspect ratio (H/D)
$\boldsymbol{c_p}$	Specific heat capacity ($\boldsymbol{J/kgK}$)
D	Diameter (m)
g	Gravitational acceleration ($\boldsymbol{m/s^2}$)
h	Heat transfer coefficient ($\boldsymbol{W/m^2K}$)
$\boldsymbol{\bar{h}}$	Average heat transfer coefficient ($\boldsymbol{W/m^2K}$)
H	Height ($\boldsymbol{m}$)
k	Thermal conductivity ($\boldsymbol{W/mK}$)
L	Characteristic length (m)
$\boldsymbol{\overline{Nu}}$	Average Nusselt number
Pr	Prandtl number
$\boldsymbol{\dot{q}_{gen}}$	Volumetric heat generation ($\boldsymbol{W/m^3}$)
$\boldsymbol{q''}$	Heat flux ($\boldsymbol{W/m^2}$)
$\boldsymbol{Q_{total}}$	Total rate of heat loss ($\boldsymbol{W}$)
$\boldsymbol{R}$	Radius ($\boldsymbol{m}$)
Ra	Rayleigh number
$\boldsymbol{Ra_{q,gen}}$	Rayleigh number (Heat generation)
T	Temperature (°C)
r	Radial position (m)
$\bar{T}$	Average temperature (°C)
V	Tank volume (m^3)
v_r	Radial component velocity (m/s)
v_z	Axial component velocity (m/s)
v_θ	Azimuth component velocity (m/s)
z	Axial position (m)

Subscripts

f	Water
w	Entire wall
b	Baffle
t	Top wall
s	Side wall
btm	Bottom wall

Greek symbols

α	Thermal diffusivity (m^2/s)
β	Volume expansion coefficient
ρ	Density (kg/m^3)
υ	Kinematic viscosity (m^2/s)

Keywords: thermal storage; heat loss; natural convection; convection suppression

*Corresponding author: timothy.anderson@aut.ac.nz

1. Introduction

One of the most critical challenges that humanity faces is to meet the growing energy demand. Given that fossil fuel reserves are limited, it is relevant to switch to renewable energy resources in order to have a sustainable society. Solar energy is recognized as one of the most promising sources because it delivers about 3.78 million EJ to the surface of the earth, which translates to 6,500 times the global energy consumption in the year 2018 [1]. The conversion of solar energy into thermal energy is highly efficient and is widely used [2], particularly for domestic water heating. However, thermal storage system is essential to preserve the collected thermal energy due to the intermittent nature of solar energy. To this end, various low temperature (<150°C) thermal energy storage (TES) systems have been examined by numerous researchers. Such systems have included sensible heat storage (SHS) [3-5], phase-change material (PCM) storage [6-8], and thermo-chemical material (TCM) storage [9-11]. Despite the superior performance promised by PCM and TCM storage systems, these technologies often require considerable amounts of energy for operation and pose challenges in their maintenance.

As a result, SHS tank with water is the most widely used TES for domestic water heating due to its low cost and high availability [5, 12]. Given that solar water heating system are easy to operate and only require simple maintenance, the total number of solar water heating systems reached approximately 105 million in 2018 [13]. This increase in the number of solar water heaters had helped to satisfy the demand of domestic hot water requirement, which accounted for 90% of global thermal energy usage [13]. Depending on how water from the tank circulates through the collector to get heated, solar domestic hot water (SDHW) systems can be classified into active and passive systems. Although the concept of passive solar water heating systems is simple and requires little maintenance, [14] showed that active solar water heating systems have higher efficiencies, their values being 35–80% over that of the passive systems in the range of 30-50%.

Unlike passive systems, water is pumped between the collector and storage tank in active solar water heating systems. In active systems, water in the storage tank can be heated by pumping it to the collector (direct circulation) or by circulating a heat transfer fluid between the collector and storage tank through the heat exchanger pipe (indirect circulation). Despite the recent developments in active indirect circulation systems, such as mantle heat exchanger encapsulating the storage tank [15], internal heat exchanger coil [16], solar combisystems with a secondary heating source [17], active direct circulation systems still remain attractive due to their simplicity, low cost and ease of maintenance.

To briefly outline, active direct circulation systems operate by circulating the water between the solar collector and storage tank to collect heat during charging (solar heating loop) while stored hot water is transferred to the load, and an equal amount of cold water is supplied usually to the bottom of the tank during discharging (load loop). This direct circulation of water leads to thermal stratification inside the storage tank where a portion of hot water with a lower density resides at the top while the cold water with higher density remains at the bottom of the tank due to buoyancy. The presence of thermal stratification inside the tank has been shown to exhibit a better overall system performance than a mixed tank during charging operation of a solar water heating system [18-21]. This is because the cold water drawn from the bottom of a stratified tank and sent to a solar collector is at a lower temperature than that of a mixed tank, which allows it to collect more thermal energy from the collector [22-26].

Over the years, extensive research has been conducted in a view of improving the degree of thermal stratification in the storage tank by varying geometrical factors such as tank aspect ratios [27, 28], tank orientation [19, 21], different types of inlet stratifiers [29-36] and baffle plates [37, 38], and operational factors such as mass flow rate and inlet temperature variation [39, 40]. More comprehensive reviews describing the effect of different parameters on thermal stratification can be found in [41-43].

Another important factor that adversely affects the performance of stratified tanks is heat loss to the ambient air, which is more pronounced during off-sunshine hours due to the lower ambient temperatures [44]. During this period, the initial temperature distribution inside a storage tank can be either in non-stratified or stratified depending on whether the tank is fully or partially charged. When the tank is fully charged, it is initially filled with hot water at a constant temperature whereas in the case of partially charged tank it is initially stratified with different levels of hot and cold water. The extent to which heat loss affects the performance varies depending on the initial temperature profile.

Knowing this, researchers have attempted to examine the effect of geometrical parameters on heat loss for both initially stratified and non-stratified tanks. Yang et al. [20] numerically investigated initially non-stratified tanks with various shapes and concluded that tanks with low surface area to volume ratio results in reduced rate of heat loss.

Miller [45] was one of the earliest studies, and investigated the effect of tank wall material (thermal conductivity) on the heat loss from an initially stratified tank. The author reported that

the rate of heat loss from a highly conductive aluminum tank was significantly higher than that from less conductive glass tank. Similarly, Armstrong et al. [46] highlighted the importance of wall thermal conductivity on performance of storage tanks. In addition, the results of the study suggested that reducing the wall thickness of a tank notably decreases the amount of serviceable hot water volume, owing to the lower conduction resistance offered by the wall. Given that tank wall material has significant influence on thermal stratification, it has been highlighted by other studies [47, 48].

Now, contemplating on the process of heat loss from stored water to the tank wall, it is evident that the principal heat transport mechanism is through natural convection inside the tank. To understand the natural convection flow inside a tank subjected to heat loss, Fan and Furbo [49] numerically studied the transient cooling of cylindrical tanks that were initially stratified. The results showed that there is a strong buoyancy driven downward flow along the side walls of the tank, and this is responsible for natural convection heat loss to the ambient.

Attempting to curtail heat loss from the tank, Shyu and Hsieh [50] numerically investigated the effect of placing insulation over the exterior and the interior of the initially stratified tank on heat loss. They concluded that when insulation is placed over the interior of the tank, heat loss to the ambient is reduced to a certain extent since the heat conducting tank wall is protected by the insulation, which suppresses the natural convection heat transfer inside the tank.

With reference to the literature, it is apparent that numerous researchers have shown great interest in reducing heat loss from storage tanks by varying their geometry. Alternatively, there appears to be the potential to reduce heat loss by attempting to suppress the natural convection flow inside the tank, which Fan and Furbo [49] highlighted as being a driver of heat loss. Although the use of baffle plates to improve the performance of solar storage tanks during charging by altering the incoming flow from the collector has been explored in the literature, the potential benefit of baffles in reducing heat loss in the absence of the external flow has not been investigated. Given that standing heat loss (in the absence of external flow) during off-sunshine hours can be extremely detrimental to thermal performance of storage tanks, the ability to control or reduce natural convection heat transfer inside a tank with passive baffles in relation to its geometrical factors could increase the overall thermal resistance to heat loss. Subsequently, this could lead to potential reductions in the amount of insulation needed or even negate the need for insulation in an ideal situation without incurring significant additional costs.

Hence, the purpose of this study is to fill the gap in the literature by investigating, in detail, the influence of baffles on the natural convection inside a vertical cylindrical storage tank.

2. Method

2.1 Geometry design

As seen in Fig. 1 (a), the tank considered in this study was developed as a three-dimensional CFD model using ANSYS FLUENT 19.2 and was equipped with a thin, cylindrical baffle jacket mounted parallel to the cylindrical side wall. This baffle configuration was chosen, as it was thought that it would 'trap' a layer of relatively stagnant fluid between the baffle and the tank wall. In turn this would direct any downward flow away from the side wall, thus reducing any heat loss directly to the outer wall. In essence, it was hoped that the tank would become somewhat 'self-insulating'.

Given that this study is a first attempt to explore the effect of baffle on natural convection in a storage tank, it is important to fully understand the influence its geometrical parameters on heat transfer independently, before incorporating the impact of its thermal conductivity. As such, the considered baffle is assumed to be adiabatic.

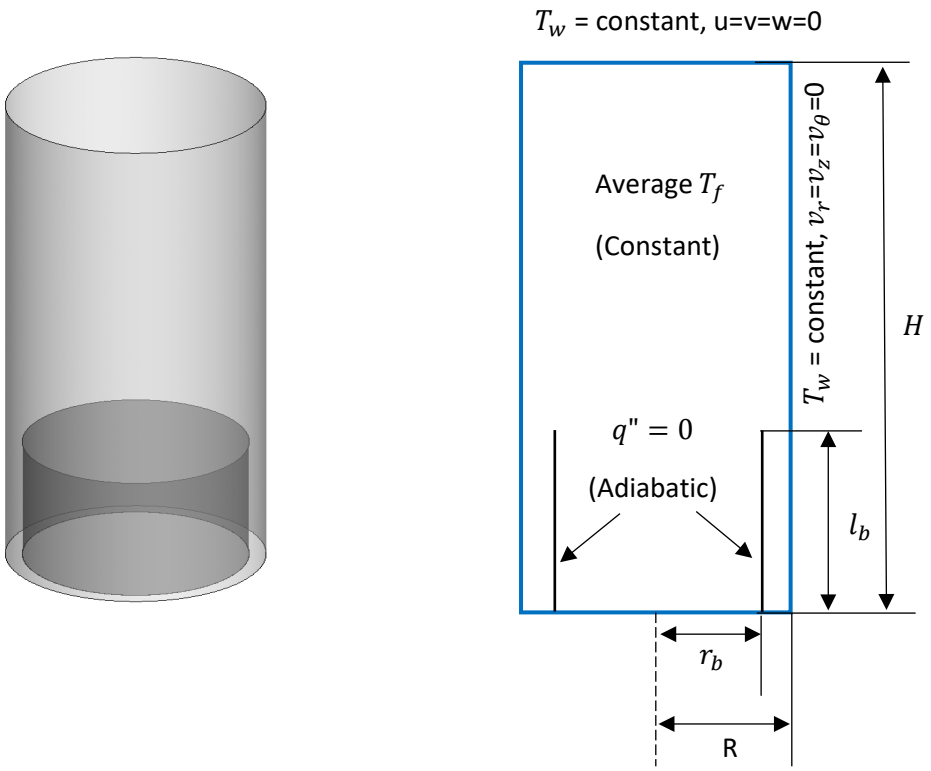

Fig. 1. (a) Baffle configuration and (b) Boundary conditions considered in the study

To examine how the proportions of such a baffling system would influence both heat transfer and flow within the tank, three radial baffle placements were considered, 6.5%, 13% and 26% of the tank radius (R-r_b). In addition, three baffle lengths were modelled, 25%, 50% and 75% of the tank height. Furthermore, two tank volumes and aspect ratios were examined, following a typical range of solar domestic hot water tank configurations as reported by [51], as shown in Table 1.

Table 1. CFD tank geometry configurations

Tank volume (V)	Aspect ratio (AR)
169 L	1
	2.3
	2.8
402 L	1
	2.3
	2.8

2.2 Boundary conditions

The effect of a baffle on the natural convection or in general, the natural convection in a storage tank can be studied using transient analysis with the inclusion of either thick tank walls or insulation to resemble a practical situation [20, 47, 50, 51]. However, the results obtained from this type of analysis are not generalizable enough to be fully applicable to different practical situations. This is because they are linked to both the elapsed cooling time from the initial state of the tank (i.e. stratified or unstratified) and the insulation thermal resistance.

Having said that, it was decided to investigate the effect of a baffle on natural convection in a storage tank using pseudo steady state analysis. This prevents the natural convection heat transfer from being linked to the cooling time that has elapsed from the initial state of the tank, and to the tank's thermal resistance. To achieve this, an energy source term was included to model the uniform volumetric generation of heat, $\dot{q}_{gen}$, which is active in the entirety of the tank including the space between the baffle and the tank wall. The rate of volumetric heat generation was not constant and varied for different tank geometries examined in this study to ensure that the average hot water temperature (T_f) was held at a constant temperature of 60˚C while the outer walls were specified to be isothermal at a lower temperature (T_w) of 59˚C, as shown in Figure 1(b). In other words, the rate of heat generation was tied to the rate of heat loss from the tank as a result of heat transfer through a finite temperature difference.

Although the inclusion of volumetric heat source is arguably different from the real system, which have external insulation and subject to convection heat loss to the ambient, this boundary condition approximates the case of a tank at rest at any given time inside which the fluid is weakly stratified, while subjected to standing heat loss. This represents a situation in which the tank has lost a certain amount heat from its fully charged state and the method has been used by several previous studies to inform our understanding of natural convection inside cylindrical enclosures [52-54].

Moreover, taking an average hot water temperature of 60˚C (since it falls within the operating conditions of solar water storage tanks) while the wall temperature is 59˚C resembles the fact that the tank wall temperature is always close to the water temperature, irrespective of the presence of insulation. As such the boundary conditions resemble those for heating at constant heat flux on the walls [55-57] and isothermal walls [58-60] for vertical storage tanks and allow us to examine the relationship between the baffle's geometric parameters and natural convection independent of simulation time and insulation-related parameters.

2.3 Flow regime

Before the CFD model could be solved, it was necessary to determine the flow regime of natural convection that takes place in the cavity. In this respect, the Rayleigh number for a storage tank with internal heat generation source, $Ra_{i,gen}$ can be defined as in Equation (2) [61].

$$Ra_{i,gen} = \frac{g\beta_f\left(\frac{\dot{q}_{gen}H^2\rho_f c_{p\,f}\alpha_f}{k_f}\right)H^3}{\upsilon_f\alpha_f} \qquad (2)$$

Referring to [51] and [62], convection heat transfer losses from the water to the wall are in the magnitude of $10^2(W/m^2K)$. Taking this into consideration, the rate of volumetric heat generation required to keep the average temperature of water at 60˚C for the considered cases would result in Rayleigh numbers, $Ra_{i,gen}$ between 10^{13} and 10^{14}. Given these findings, it was necessary to consider turbulence modelling within the tank [63]. As such, two-equation low-Re turbulent LB model was chosen because low-Re turbulent models were proven to be suitable for provide reasonable estimates for resolving turbulent behavior of flow inside volumetrically heated liquid pools [61].

2.4 Governing equations

The steady state three-dimensional CFD model can be solved using the continuity, momentum, energy and low-Re k-epsilon LB model as shown in Equations (3) – (8).

Continuity equation:

$$\nabla.(\rho\vec{v}) = 0 \tag{3}$$

where $\vec{v}$ is the velocity vector.

Momentum equation:

$$\nabla.(\rho\vec{v}\vec{v}) = -\nabla p + \nabla.\tau + \rho\vec{g} \tag{4}$$

where $\rho\vec{g}$ is the gravitational body force, p is the static pressure and τ is the viscous stress.

Energy equation:

$$\nabla.(\rho\vec{v}E) = \nabla.(k\nabla T) + S_h \tag{5}$$

where E denotes the sensible enthalpy and S_h denotes the volumetric heat source, which was included as uniform volumetric generation of heat, $\dot{q}_{gen}$ in this study.

Turbulence equations:

$$\nabla.(\rho k\vec{v}) = \nabla.\left[\left(\mu + \frac{\mu_t}{\sigma_k}\right)\nabla\mathrm{k}\right] + P_k - \rho\varepsilon \tag{6}$$

$$\nabla.(\rho\varepsilon\vec{v}) = \nabla.\left[\left(\mu + \frac{\mu_t}{\sigma_\varepsilon}\right)\nabla\varepsilon\right] + C_1 f_1 \frac{\varepsilon}{k} P_k - C_2 f_2 \rho \frac{\varepsilon^2}{k} + D_\varepsilon \tag{7}$$

$$\mu_t = \rho C_\mu f_\mu \frac{k^2}{\varepsilon} \tag{8}$$

where C_1, C_2 and C_μ are constants, μ_t is the turbulent viscosity, P_k and D_ε denote the generation and dissipation of turbulent kinetic energy due to mean velocity gradients, σ_k and σ_ε are the turbulent Prandtl numbers for k and ε, respectively. A detailed calculation of parameters f_1, f_2 and f_μ involved in low Re k-epsilon LB model can be found in [62].

2.5 Solving procedure

To accelerate the convergence of the calculation, the pressure-velocity coupling was handled using a coupled algorithm, since it offers a robust solution for steady state flows. Interpolation of pressure was resolved using a body-force weighted algorithm, and the convective terms were interpolated using a second-order upwind scheme [64]. Given the small temperature changes of water inside the tank, the Boussinesq approximation was applied for the treatment of density

variation in the momentum equation. In solving the governing equations, the solution was considered to be fully converged when the residuals of all equations fell below 10^{-4}.

2.6 Grid independence analysis

To reduce the computational effort, without compromising the accuracy of CFD results, it was necessary to carry out a mesh sensitivity analysis. For the analysis, the natural convection heat transfer coefficient on the side wall of the tank was used to assess the suitability of different mesh sizes. Given the variation of geometry in the current study, it was decided to perform mesh sensitivity analysis for two tanks, 169L with an aspect ratio of 1 and a 402L with aspect ratio of 2.8, both having a fixed baffle placed at 13% of tank radius $(R - r_b)$ with the length of the baffle being 25% of the tank height. Fig. 2 shows the change in the natural convection heat transfer coefficient on the tank side wall for different tank geometries and element sizes. From the results, it is apparent that reducing the element size smaller than 7.5 mm did not result in notable changes in heat transfer coefficient. As such, an element size of 7.5 mm was chosen for this study.

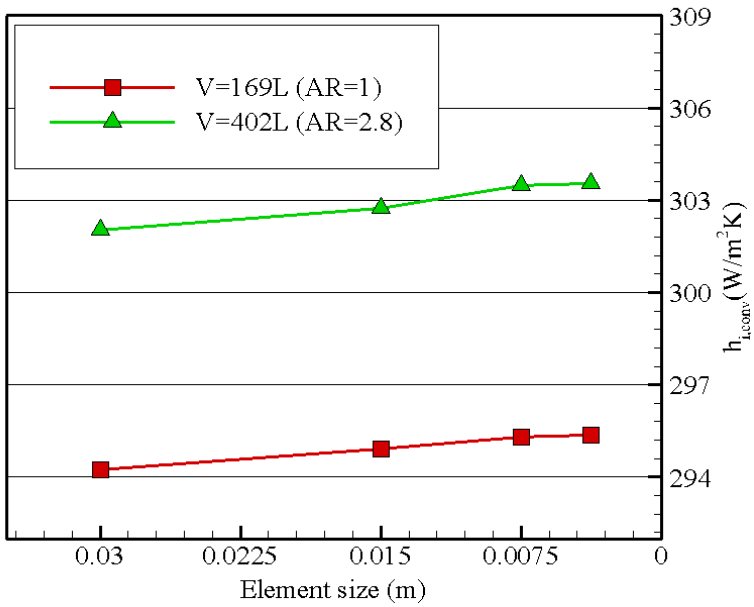

Fig. 2. Changes in natural convection heat transfer coefficient with element size for two tank geometries with same baffle configuration ($R - r_b = 0.013R$ and $l_b = 0.25H$)

2.7 Calculation of local and average Nusselt numbers

The representation of how baffles can reduce natural convection was achieved by the average Nusselt number of the entire tank (top, side and bottom walls) and the local Nusselt number of each tank wall. The values of both local and average Nusselt numbers were extracted from FLUENT. To demonstrate how FLUENT calculates the local Nusselt number on each wall, its calculation on the tank side wall is shown in Equations (9) – (12).

Side Wall:

$$\bar{T}_f = \frac{1}{\pi R^2 H}\int_0^R \int_0^H 2\pi r\, T\, dz\, dr, \qquad \bar{T}_w = \frac{1}{H}\int_0^H T_{|r=R}\, dz \tag{9}$$

$$q_s'' = \frac{1}{H}\mathrm{k}\int_0^H \frac{\partial T_f}{\partial r}_{|r=R}\, dz \tag{10}$$

$$h_s = \frac{q_s''}{(\bar{T}_f - \bar{T}_{w,s})} \tag{11}$$

$$Nu_s = \frac{h_s \mathrm{H}}{\mathrm{k}} \tag{12}$$

where, $\bar{T}_f$ is the average temperature of the fluid, $\bar{T}_{sw}$ is the average temperature of the side wall, q_s'' is the average heat flux on the side wall, h_s is the local heat transfer coefficient on the side wall, k is the thermal conductivity of water, Nu is the local Nusselt number on the sidewall.

The calculation of the average Nusselt number on the entire tank wall is indicated in Equation (13)-(17).

$$\bar{T}_w = \frac{A_t\bar{T}_t + A_s\bar{T}_s + A_{btm}\bar{T}_{btm}}{A_{total}} \tag{13}$$

$$\bar{T}_t = \frac{1}{\pi R^2}\int_0^R T_{|z=H}\, 2\pi r\, dr, \qquad \bar{T}_{btm} = \frac{1}{\pi R^2}\int_0^R T_{|z=0}\, dr \tag{14}$$

$$Q_{total} = A_t q_t'' + A_s q_s'' + A_b q_{btm}'', \qquad A_{total} = A_t + A_s + A_{btm} \tag{15}$$

$$\bar{h} = \frac{Q_{total}}{A_{total}(\bar{T}_f - \bar{T}_w)} \tag{16}$$

$$L_c = \frac{V}{A_{total}} \tag{17}$$

$$\overline{Nu} = \frac{\bar{h}L_c}{k} \tag{18}$$

where, $\bar{T}_w$ is the average temperature of the tank wall, $\bar{T}_t$ and $\bar{T}_{btm}$ are the average temperatures of the top and bottom walls, q_t'' and q_b'' are the average heat fluxes on the top and bottom walls, Q_{total} is the rate of heat loss from the entire tank, A_t, A_s and A_b are the surface area of the top, side and bottom walls, A_{total} is the total surface area of tank walls, $\bar{h}$ is the average heat transfer coefficient, V is the volume of the tank, L is the characteristic length, $\overline{Nu}$ is the average Nusselt number on the entire tank wall.

2.8 Validation

Having developed the simulation methodology, experimental data obtained from [63] was used as a benchmark to validate the results from computational simulations of a tank without a baffle

jacket due to lack of experimental data with baffled tanks, as indicated in Table 2. In their study, [65] investigated steady state cooling of rectangular tank with uniform heat generation having Rayleigh numbers, $Ra_{q,gen}$ between 5×10^{12} and 10^{14}. However, it has been shown that the results from rectangular tanks are applicable to cylindrical tanks and are unlikely to result in significant variations in computational solutions, so long as the condition shown in Equation (3) is met [66]. In this respect, all the investigated cases shown in Table 1 were found to fulfill this condition.

$$D \geq \frac{35H}{(\frac{Ra}{Pr})^{\frac{1}{4}}} \tag{19}$$

From Figure 3, it is apparent that the simulated CFD results agrees well with the published data [65] with the maximum variation found to be within 15%. On this basis it is believed that the validated computational methodology will be sufficient for investigating the effect of baffle on natural convection heat transfer given that a similar approach has been used in previous studies [67, 68].

Table 2. Chosen validation points along with dimensions of CFD models considered

H (m)	AR	Volume (L)	$\dot{q}_{gen}(W/m^3)$	$Ra_{q,gen}$
0.5	1	125	2000	6.28×10^{12}
0.52	1	140	2000	7.64×10^{12}
0.55	1	157	2000	1.01×10^{13}
0.6	1	216	2000	1.56×10^{13}
0.63	1	250	2000	1.99×10^{13}
0.8	1	512	2000	6.58×10^{13}

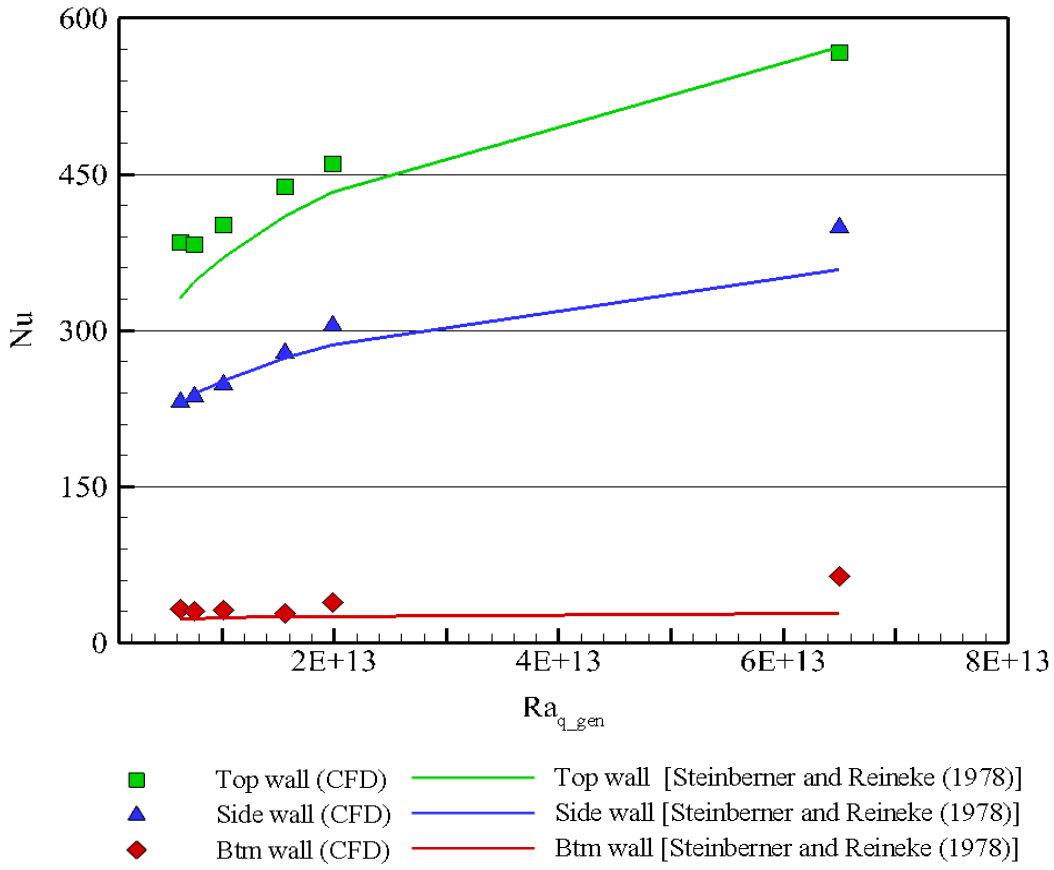

Fig. 3. Validation of CFD model with published Nusselt correlations on top, side, and bottom walls

3. Results and Discussion

Having validated the computational methodology, it was decided to explore the effect of baffle length and its location on natural convection heat transfer inside storage tanks having various volumes and aspect ratios shown in Table 1.

3.1 Effect of baffle length on natural convection flow

The perceived benefit of placing a considered baffle configuration inside the tank was to divert the sinking boundary layer flow towards the inner side of the baffle away from the side wall. In Figure 4, it can be seen that the longest baffle placed closest to the side wall appears to achieve this to a certain extent. This is due to the presence of a stratified region between the baffle and the side wall that is more apparent in Figure 5. In this jacket, the velocity of the boundary layer flow is also noticeably reduced compared to the tank without the baffle. It is important to note however that this flow behavior was achieved with the assumption that baffle jacket is adiabatic with no conduction heat transfer across it.

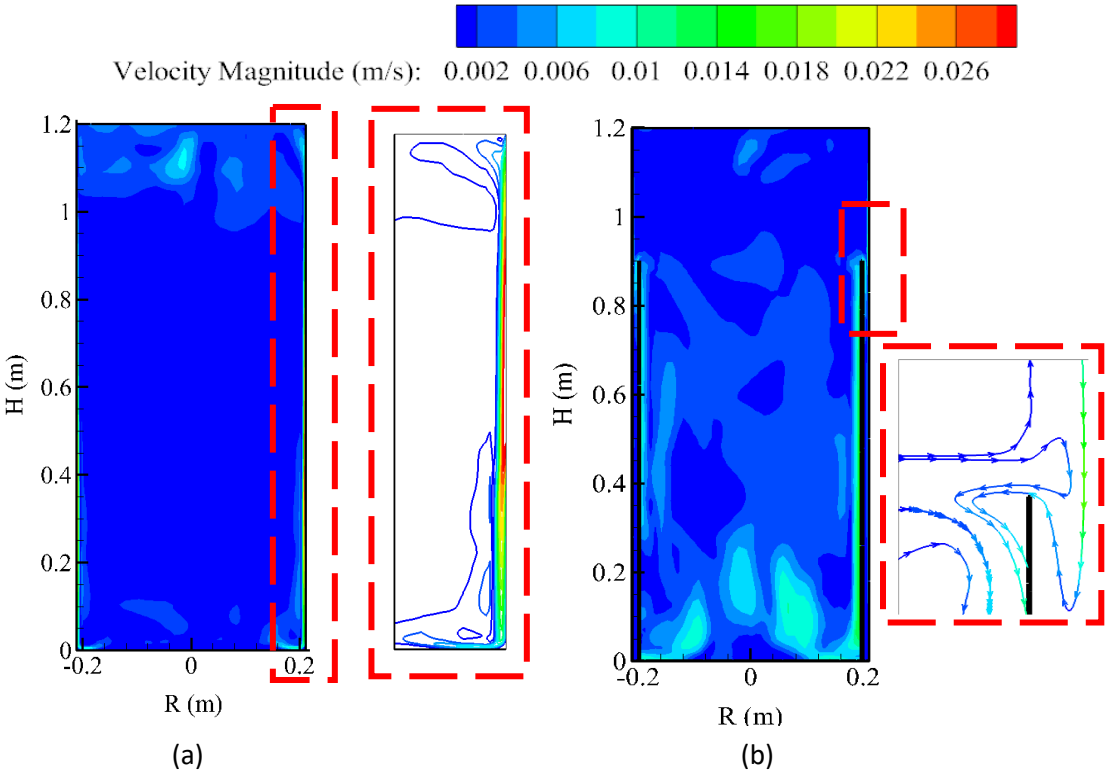

Fig. 4. Velocity contours for tank model (V=169L, AR=2.8) at the center plane with (a) no baffle and (b) baffle ($(R-r_b)/R=0.065$, $l_b/H=0.75$)

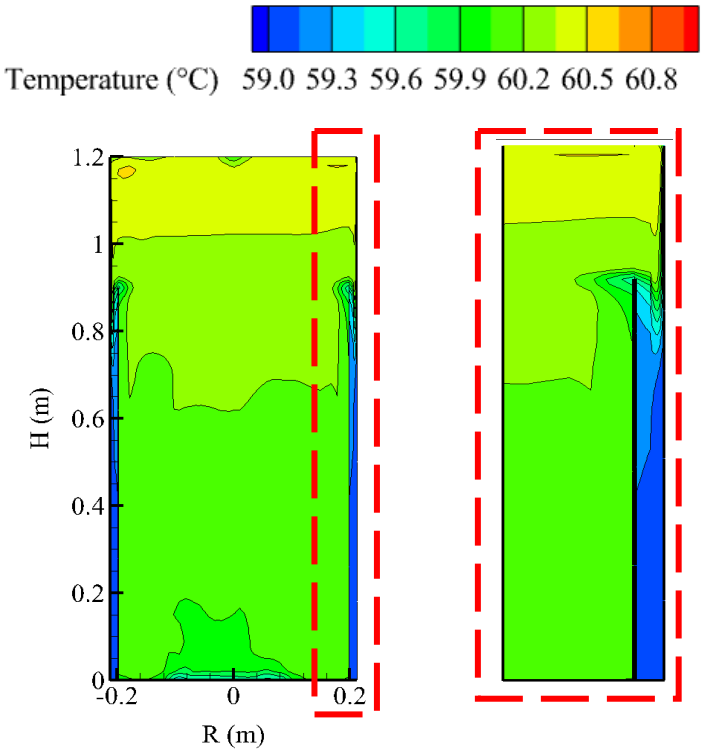

Fig. 5. Temperature contour for tank model (V=169L, AR=2.8) at the center plane with baffle ($(R-r_b)/R=0.065$, $l_b/H=0.75$)

Similarly, in Figure 6, it is apparent that baffles with shorter lengths, 50% and 25% of the height, were still able to redirect the boundary layer flow away from the side wall. However, it was also observed that shortening the length of the baffle allows boundary layer to grow and reach higher velocity in comparison to that of longest baffle (Figure 4 (b)) which could potentially enhance convection heat transfer inside the tank.

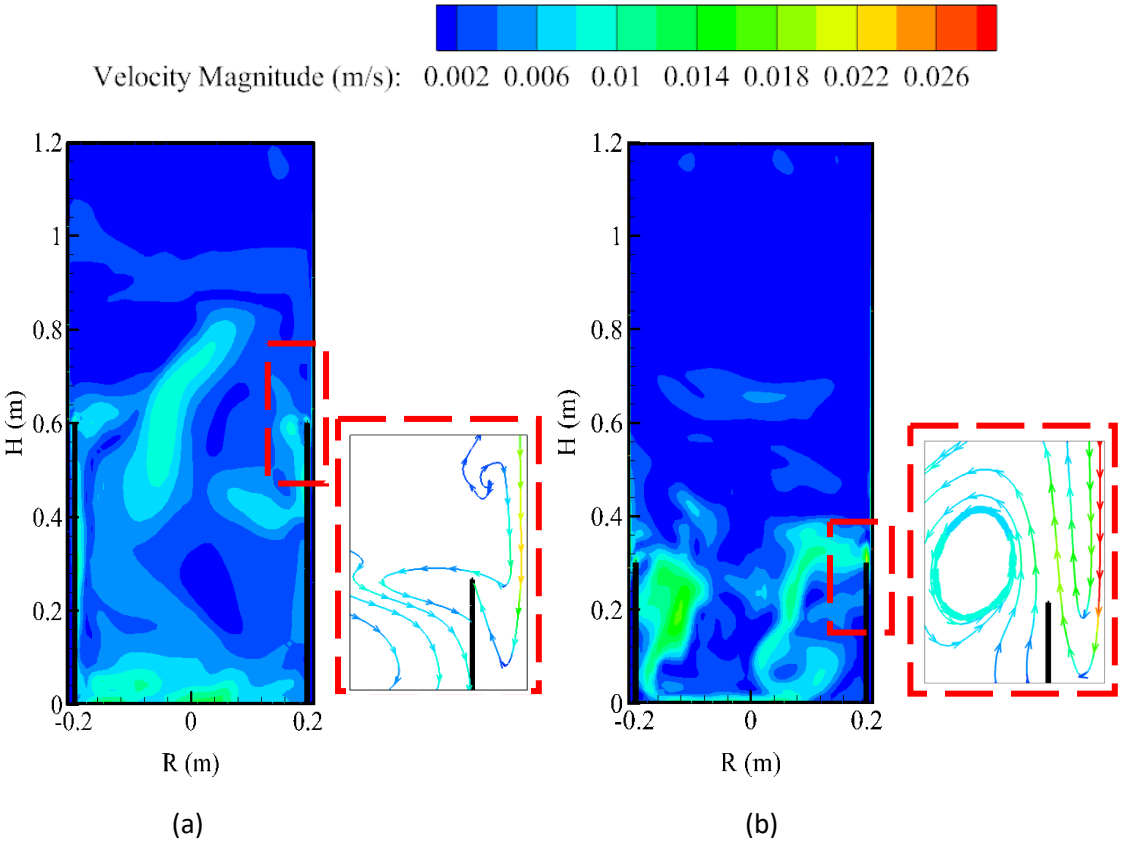

Fig. 6. Velocity contours for tank model (V=169L, AR=2.8) at the center plane with: (a) baffle ((R- r_b)/R=0.065, l_b /H=0.5) and (b) baffle ((R- r_b)/R=0.065, l_b /H=0.25)

3.2 Effect of baffle position on natural convection flow and heat transfer

The position of the baffle jacket also plays an important role in limiting the natural convection flow inside the tank. Figure 7 shows the velocity contours of different baffle positions for a fixed medium baffle length (50% of tank height). It can be seen from the figure that increasing the distance between the baffle and the side wall allows the boundary layer flow (thermal plume) to progress further along the side wall. This is because the boundary layer thickness is

much thinner than the gap between the baffle and the side wall. This could potentially lead to an increase in convection heat transfer.

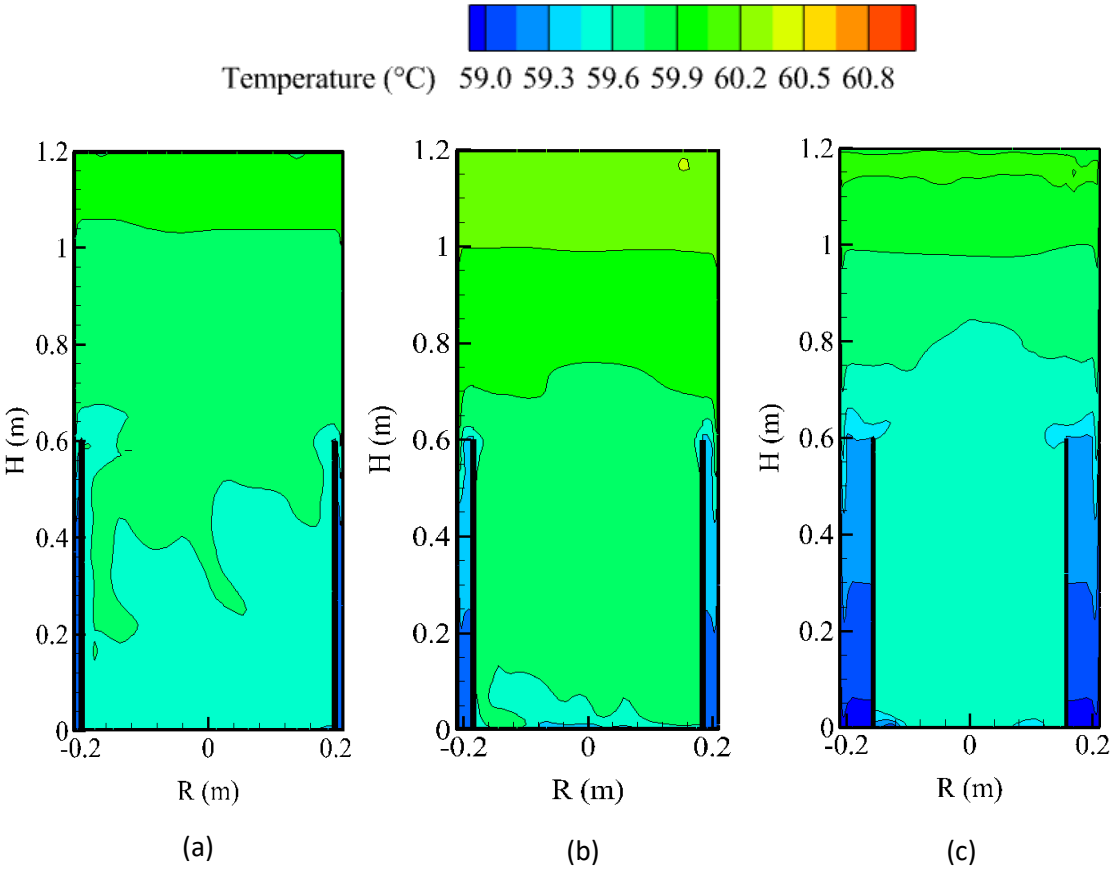

Fig. 7. Temperature contours of tank model (V=169L, AR=2.8) with different baffle positions (a) (R- r_b)/R=0.065, (b) (R-r_b)/R=0.13 and (c) (R- r_b)/R=0.26 for a fixed baffle length of l_b /H=0.5

By diverting the boundary layer flow, and preventing it from flowing along the side wall, there is a marked decrease in convection heat transfer, as represented by the Nusselt number in Figure 8. Here, it can be seen that all baffle configurations result in lower convection heat transfer when compared to the tank without a baffle.

In addition, the Nusselt number decreases with increasing baffle length since the growth of boundary layer and its velocity is proportional to the baffle length. Similarly, moving the baffle jacket away from the side wall results in higher Nusselt number since the gap between the two allows the boundary layer flow to lose heat to the side wall as it travels along the wall.

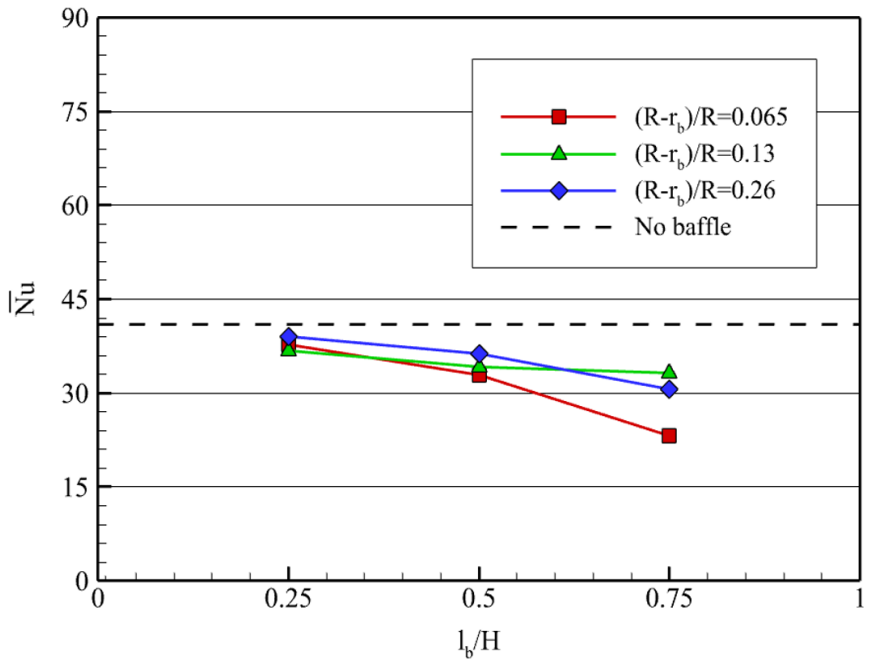

Fig. 8. Variation of overall Nusselt number with different baffle lengths and positions (V=169L, AR=2.8)

Interestingly, the Nusselt number in the case with the shortest baffle length (25% of tank height), placed at 6.5% of tank radius from the side wall was higher than that of 13%. To explain this, velocity contours of both cases were examined in greater detail. In Figure 9, it can be seen that placing a baffle close to the wall results in a recirculation cell near the top of the baffle, while this cell is absent when the baffle is placed further from the side wall (13% of tank radius). The presence of this recirculation flow marginally increases convection heat transfer on the side wall while the other tank walls remain unaffected, as shown in Figure 10. The formation of this recirculation cell could be associated with the perturbation of the boundary layer flow when it meets the baffle, due to the small gap between the baffle and the side wall relative to the boundary layer thickness.

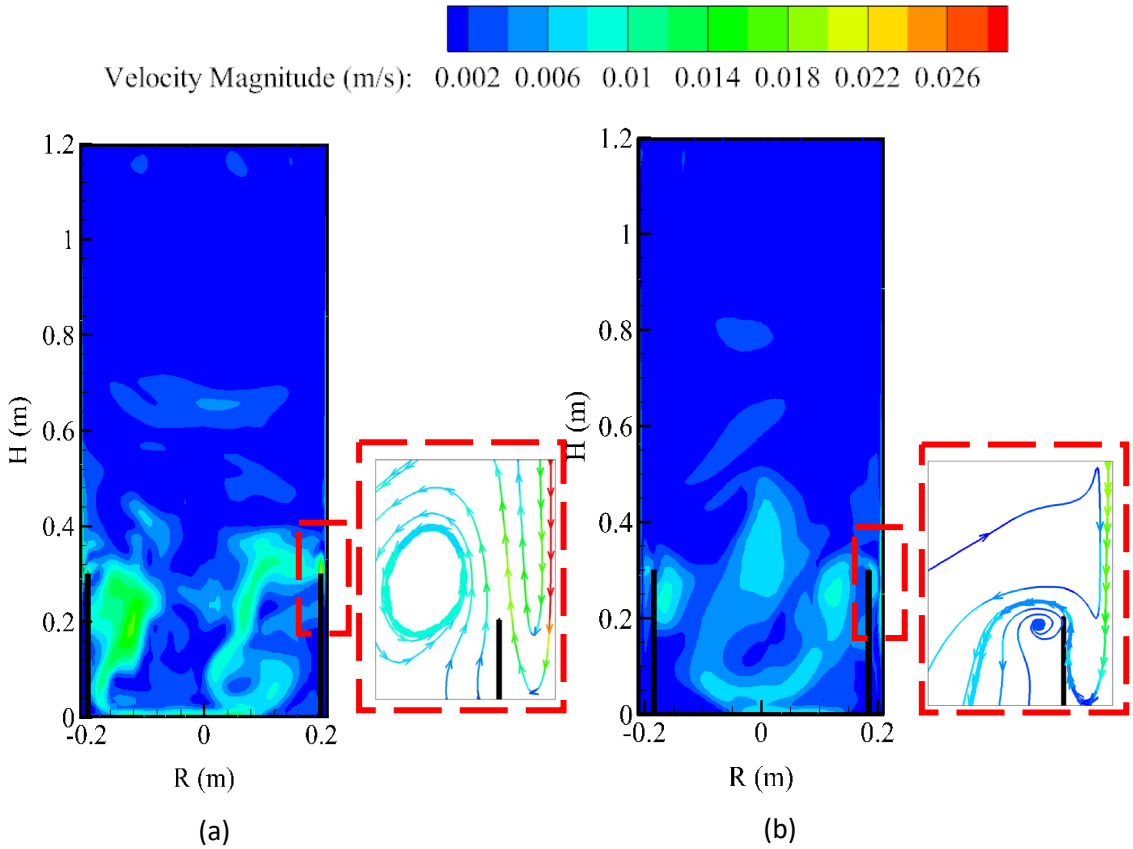

Fig. 9. Velocity contours of tank model (V=169L, AR=2.8) with different baffle positions (a) $(R- r_b)/R=0.065$ and (b) $(R- r_b)/R=0.13$ for a fixed baffle length of $l_b /H=0.25$

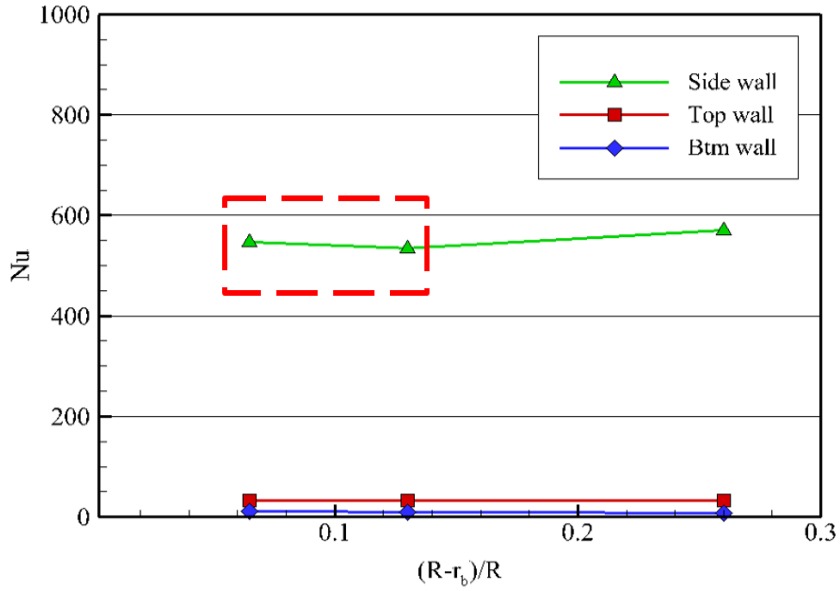

Fig. 10. Variation of convective heat transfer coefficient on each wall for different baffle positions for a fixed baffle length ($l_b /H=0.25$)

From Figure 8, it was also worth noting that the Nusselt number in the case with longest baffle length (75% of tank height), placed at 13% of tank radius from the side wall was higher than that of 26%. To explain this, velocity contours of both cases are shown in Figure 11.

In Figure 11, it is apparent that the majority of the boundary layer flow is redirected along the inner baffle wall without getting cooled by the exterior wall, leading to the formation of recirculation cells at the bottom. Because of this, a portion of the existing hot water rises and meets with the falling boundary layer near the top end of the baffle. This increases the temperature of water inside the boundary layer which leads to an increase in its velocity. However, the increase in the velocity of the boundary layer is more pronounced when the baffle is placed at 13% of tank radius from the side wall compared to that of 26%. This is because placing the baffle further away from the wall (26% of tank radius) allows part of the boundary layer flow to continue travelling along the side wall instead of getting diverted into the baffle jacket, resulting in weak recirculation cells compared to when baffle is placed nearer to the wall (13% of tank radius). This phenomenon affects convection heat transfer on the side wall while other tank walls remain unaffected, as represented by Nusselt number for each wall in Figure 12.

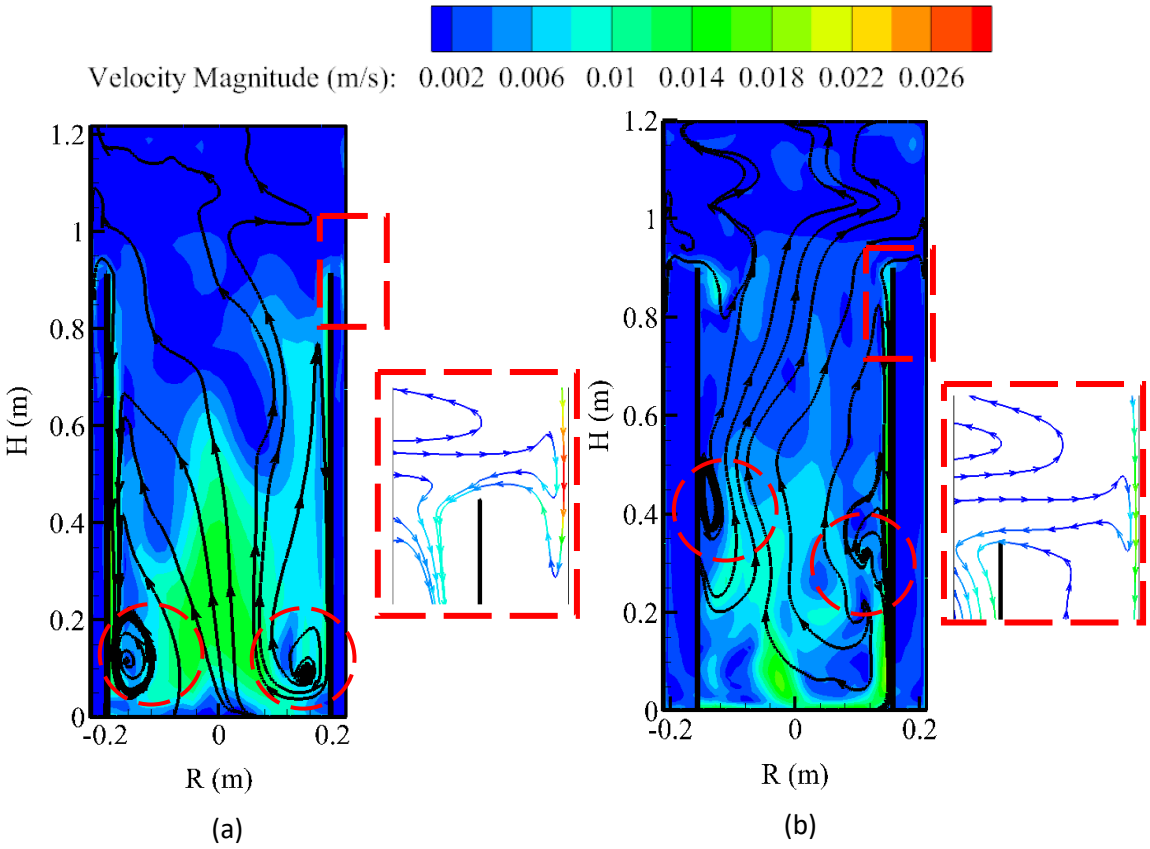

Fig. 11. Velocity contours of tank model (V=169L, AR=2.8) with different baffle positions (a) (R- r_b)/R=0.013 and (b) (R- r_b)/R=0.26 for a fixed baffle length of l_b /H=0.75

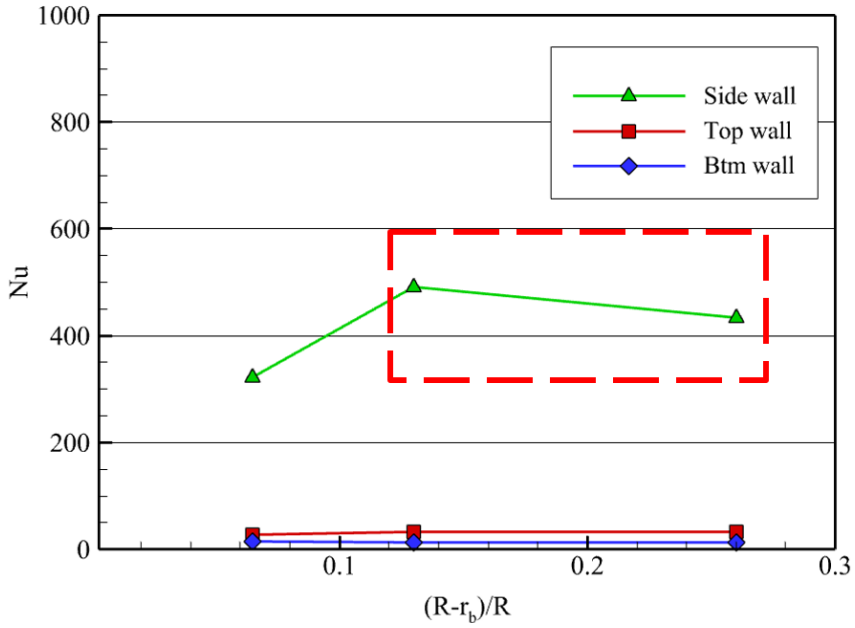

Fig. 12. Variation of convective heat transfer coefficient on each wall for different baffle positions for a fixed baffle length (l_b /H=0.75)

A similar variation in Nusselt number with baffle length and position was found for the larger tank model with 402 L and aspect ratio of 2.8, as shown in Figure 13.

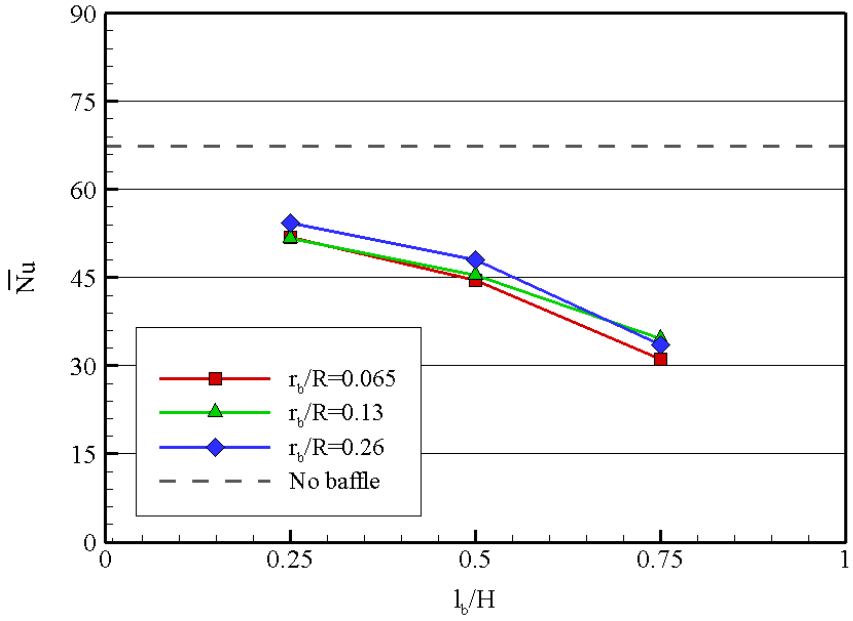

Fig. 13. Variation of overall Nusselt number with different baffle lengths and positions (V=402L, AR=2.8)

3.3 Effect of aspect ratio on natural convection heat transfer

After analyzing the effect of baffle configuration on natural convection inside the storage tanks, it was decided to examine the influence of aspect ratio on natural convection heat transfer inside these tanks. From Figure 14, it can be seen that increasing the aspect ratio decreases natural convection heat transfer inside the tank as indicated by the reduction in Nusselt number.

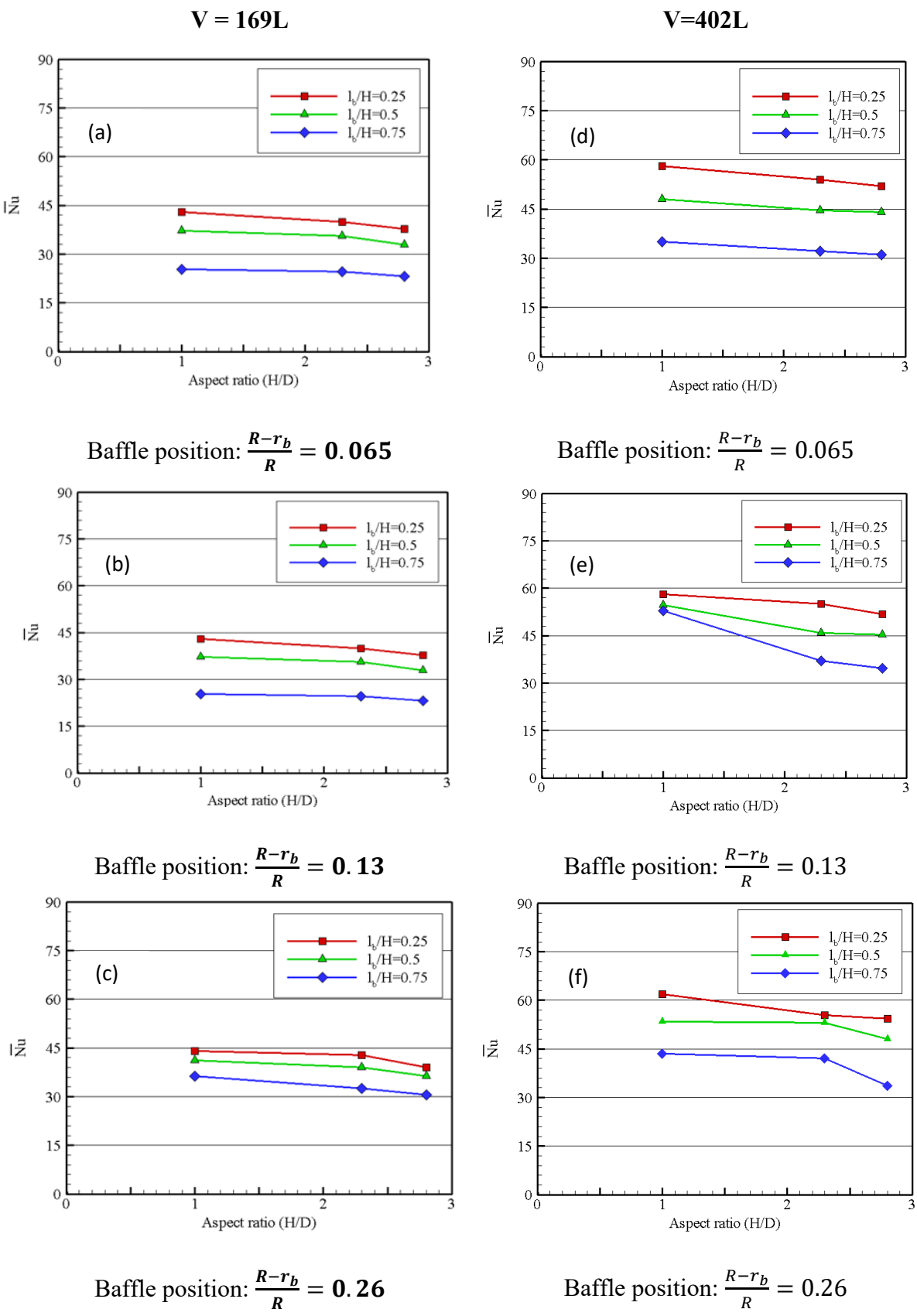

Fig. 14. Effect of aspect ratio on natural convection heat transfer for different baffle configurations for tank volumes of 169L (left) and 402L (right)

To explain this, velocity contours of the tank model with baffle length (25% of tank height) placed at a distance of 13% of tank radius from the side wall are shown in Figure 15. As can be seen from the figure, the portion of buoyancy driven boundary layer flow on the side wall directed towards the core of the tank, away from the side wall, increases with increasing aspect ratio. For aspect ratios of 1 and 2.3, the recirculation cell was observed on the inner side of the baffle owing to small portion of boundary layer flow that is redirected by the baffle. However, this recirculation flow disappears as an increasing portion of boundary layer flow is redirected away from the side wall inside the tank with aspect ratio of 2.8. This is due to an increase in the momentum of the boundary layer flow with aspect ratio, which gets disturbed by the presence of the baffle and forced to enter the inner side of the baffle. This results in a decrease in convection heat transfer on the side wall, as shown in Figure 16 (a).

On the other hand, thermal stratification inside the tank proportionally increases with aspect ratio, as indicated in Figure 16 (b). As a result, natural convection heat transfer on the top wall gets also restricted with increasing aspect ratio, leading to a decrease in convection heat transfer coefficient (see Figure 16 (a)). However, no notable natural convection on the bottom wall was observed. Similar changes flow behavior was observed in remaining tank models with different baffle configurations, thus leading to a decrease in Nusselt number with increasing aspect ratio.

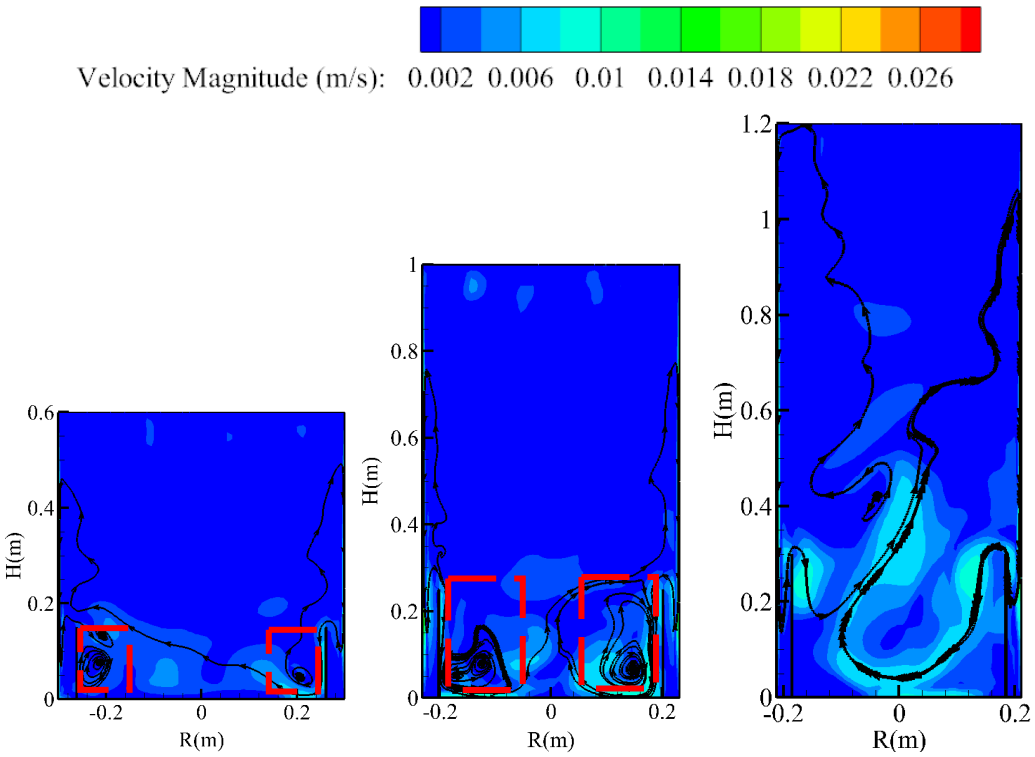

Fig. 15. Velocity contours of tank models (V=169L) with aspect ratios of (a) AR=1, (b) AR=2.3 and (c) AR=2.8 for a fixed baffle length of l_b /H=0.25 and position of (R-r_b)/R=0.013

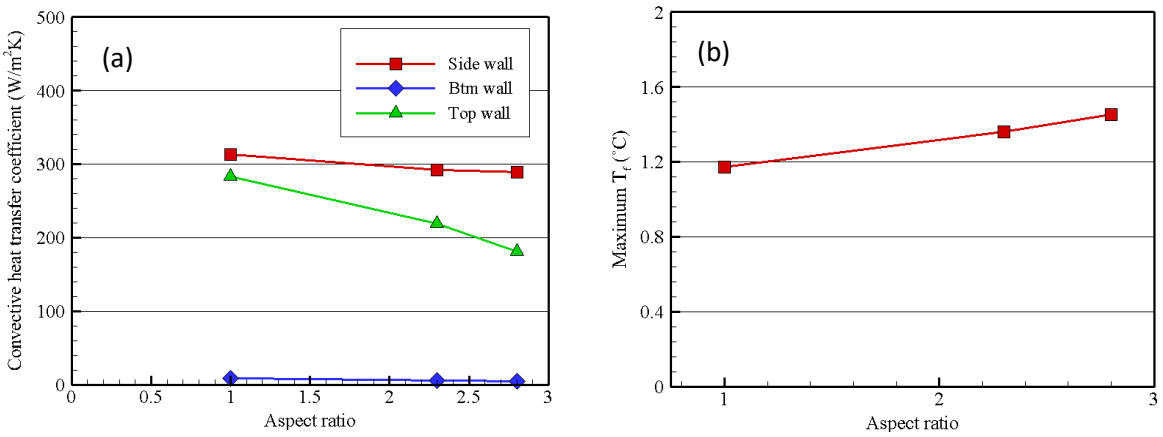

Fig. 16. (a) Variation of local convective heat transfer coefficient on each tank wall and (b) Maximum temperature difference inside the tank for tank model (V=169L) with a baffle length of l_b /H=0.25 and position of (R- r_b)/R=0.013

3.4 Correlating geometrical parameters to natural convection heat transfer

Based on the discussion in previous sections, the position and length of baffle jacket and the storage tank geometry have a direct influence on the magnitude of natural convection heat transfer inside the tank, and this is linked to the flow in the tank. To present the findings obtained from numerical CFD modelling in a generalizable way, it was decided to establish a

correlation that describes natural convection heat transfer coefficient inside vertical cylindrical storage tanks as a function of baffle jacket and tank geometries.

The obtained correlation between Nusselt number and the geometrical parameters affecting heat transfer inside the tank can be described by Equation (20):

$$\overline{Nu} = 0.354\ \mathrm{Ra}^{0.259} \left(\frac{H}{D}\right)^{-0.035} \left(\frac{l_b}{H}\right)^{-0.291} \left(\frac{R-r_b}{R}\right)^{0.054} \quad (20)$$

Where: $2.89 \times 10^7 < \mathrm{Ra} < 1.24 \times 10^8$, $1 < AR < 2.83$; $0.25H < l_b < 0.75H$, $0.74R < r_b < 0.935R$.

The Rayleigh number for natural convection inside the tank, Ra was defined based on the difference between the average temperature of water and the tank wall, as indicated in Equation (21).

$$Ra = \frac{g\beta_f(T_f - T_w)L_c^3}{\upsilon_f \alpha_f} \quad (21)$$

In Figure 17, the fitted Nusselt number correlation using multiple non-linear regression is plotted against the simulated Nusselt number. As can be seen from the figure, the proposed Nusselt correlation shows a good agreement with numerical data, with all data falling between ±15% of the simulated data. This implies that the developed correlation is suitable to estimate heat transfer coefficient for the given range of aspect ratio, baffle position and length.

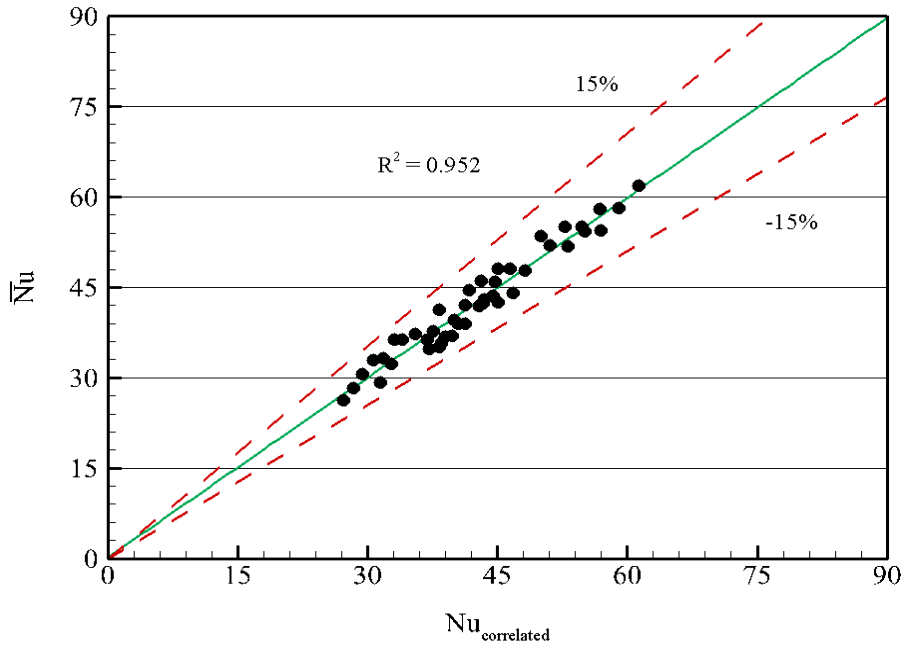

Fig. 17. Correlation of convective heat transfer coefficient inside cylindrical tanks with baffles indicating the goodness of fit

4. Conclusion

In this study, the effect of passive baffle length and position on natural convection heat transfer inside vertical cylindrical solar storage tank geometries with a range of aspect ratios was comprehensively investigated.

The findings show that the presence of a baffle inside the tank had a significant effect on natural convection through the alteration of flow. In some cases, the baffle leads to a reduction in the Nusselt number inside the tank of almost 40%. It was found that the length of the baffle is inversely proportional to the strength of natural convection inside the tank while placing the baffle closer to the side wall suppresses natural convection heat loss by diverting the boundary layer flow away from the wall.

As a result, the results show that baffle jacket having the highest length and placed nearest to the side wall leads to lowest natural convection heat transfer inside the tank. However, the material of the baffle needs to be chosen carefully, and materials with low thermal conductivity are preferable, as these avoid heat conduction through the baffle. Finally, a generalized correlation that can be used to predict natural convection heat transfer inside tanks equipped with baffle jacket was presented. It is hoped that designers of these systems can take advantage of the obtained correlation to improve the thermal performance of these tanks with a passive baffle in the future. It is also recommended to extend the study by considering strongly stratified tanks to represent more practical scenarios in the future.

References

1. Kober, T., et al., *Global energy perspectives to 2060 – WEC's World Energy Scenarios 2019.* Energy Strategy Reviews, 2020. 31: p. 100523.
2. Sadhishkumar, S. and T. Balusamy, *Performance improvement in solar water heating systems—A review.* Renewable and Sustainable Energy Reviews, 2014. 37: p. 191-198.
3. Paksoy, H., A. Snijders, and L. Stiles. *State-of-the-art review of aquifer thermal energy storage systems for heating and cooling buildings*. in *Proceedings of the EFFSTOCK conference, Stockholm, Sweden*. 2009.
4. Bauer, D., et al., *German central solar heating plants with seasonal heat storage.* Solar Energy, 2010. 84(4): p. 612-623.
5. Basecq, V., et al., *Short-term storage systems of thermal energy for buildings: a review.* Advances in Building Energy Research, 2013. 7(1): p. 66-119.
6. Gunasekara, S.N., et al., *Polyols as phase change materials for surplus thermal energy storage.* Applied Energy, 2016. 162: p. 1439-1452.
7. del Barrio, E.P., et al., *Characterization of different sugar alcohols as phase change materials for thermal energy storage applications.* Solar Energy Materials Solar Cells, 2017. 159: p. 560-569.

8. Galazutdinova, Y., et al., *Novel inorganic binary mixture for low-temperature heat storage applications.* International journal of Energy Research, 2017. 41(14): p. 2356-2364.
9. Kerskes, H., et al., *Chemical energy storage using reversible solid/gas-reactions (CWS)–results of the research project.* 2012. 30: p. 294-304.
10. N'Tsoukpoe, K.E., et al., *A systematic multi-step screening of numerous salt hydrates for low temperature thermochemical energy storage.* 2014. 124: p. 1-16.
11. Donkers, P., et al., *A review of salt hydrates for seasonal heat storage in domestic applications.* 2017. 199: p. 45-68.
12. Sarbu, I. and C. Sebarchievici, *A Comprehensive Review of Thermal Energy Storage.* Sustainability, 2018. 10(1): p. 191.
13. Weiss, W. and M. Spörk-Dür, *Solar Heat Worldwide, Global market development and trends in 2019.* IEA Solar Heating & Cooling Programme, 2020.
14. Khalifa, A.-J.N., *Forced versus natural circulation solar water heaters: A comparative performance study.* Renewable Energy, 1998. 14(1): p. 77-82.
15. Li, Q., et al., *Thermal stratification in a solar hot water storage tank with mantle heat exchanger.* Renewable Energy, 2021. 173: p. 1-11.
16. Li, A., et al., *Effects of different thermal storage tank structures on temperature stratification and thermal efficiency during charging.* Solar Energy, 2018. 173: p. 882-892.
17. Heier, J., et al., *Combining thermal energy storage with buildings–a review.* 2015. 42: p. 1305-1325.
18. Gopalakrishnan, N. and S.S. Murthy, *Mixed convective flow and thermal stratification in hot water storage tanks during discharging mode.* Applied Solar Energy, 2009. 45(4): p. 254-261.
19. Abdelhak, O., H. Mhiri, and P. Bournot. *CFD analysis of thermal stratification in domestic hot water storage tank during dynamic mode*. in *Building Simulation*. 2015. Springer.
20. Yang, Z., et al., *Comparative study of the influences of different water tank shapes on thermal energy storage capacity and thermal stratification.* Renewable Energy, 2016. 85: p. 31-44.
21. Kurşun, B. and K. Ökten, *Effect of rectangular hot water tank position and aspect ratio on thermal stratification enhancement.* Renewable Energy, 2018. 116: p. 639-646.
22. Sheridan, N., K. Bullock, and J. Duffie, *Study of solar processes by analog computer.* Solar Energy, 1967. 11(2): p. 69-77.
23. Gutierrez, G., et al., *Simulation of forced circulation water heaters; effects of auxiliary energy supply, load type and storage capacity.* Solar Energy, 1974. 15(4): p. 287-298.
24. Fischer, L., A. Dijkmans, and C. van Koppen. *Stratification effects in the short and long term storage of solar heat*. in *Sun: mankind's future source of energy: proceedings of the International Solar Energy Society congress, New Delhi, January 1978*. 1978. Pergamon.
25. Han, S., S. Wu, and D. Christensen, *Effects of thermal stratification in water storage tank for the performance of a solar hot water system*. 1978, Alabama Univ., Huntsville (USA).
26. Sharp, M. and R. Loehrke, *Stratified thermal storage in residential solar energy applications.* Journal of Energy, 1979. 3(2): p. 106-113.
27. Lavan, Z. and J. Thompson, *Experimental study of thermally stratified hot water storage tanks.* Solar Energy, 1977. 19(5): p. 519-524.

28. Ievers, S. and W. Lin, *Numerical simulation of three-dimensional flow dynamics in a hot water storage tank.* Applied Energy, 2009. 86(12): p. 2604-2614.
29. Shah, L.J., E. Andersen, and S. Furbo, *Theoretical and experimental investigations of inlet stratifiers for solar storage tanks.* Applied thermal engineering, 2005. 25(14-15): p. 2086-2099.
30. Andersen, E., et al., *Investigations on stratification devices for hot water heat stores.* International journal of Energy Research, 2008. 32(3): p. 255-263.
31. Lohse, R., et al. *Optimization of a stratification device for thermal storage tanks*. in *11th International Conference on Thermal Energy Storage, Effstock, Stockholm*. 2009.
32. García-Marí, E., et al., *A new inlet device that enhances thermal stratification during charging in a hot water storage tank.* Applied Thermal Engineering, 2013. 61(2): p. 663-669.
33. Dragsted, J., et al., *Thermal stratification built up in hot water tank with different inlet stratifiers.* Solar Energy, 2017. 147: p. 414-425.
34. Moncho-Esteve, I.J., et al., *Simple inlet devices and their influence on thermal stratification in a hot water storage tank.* Energy and Buildings, 2017. 150: p. 625-638.
35. Wang, S. and J.H. Davidson, *Performance of a rigid porous-tube stratification manifold in comparison to an inlet pipe.* Solar Energy, 2017. 146: p. 298-308.
36. Wang, Z., et al., *The thermal stratification characteristics affected by a novel equalizer in a dynamic hot water storage tank.* Applied Thermal Engineering, 2017. 126: p. 1006-1016.
37. Altuntop, N., et al., *Effect of obstacles on thermal stratification in hot water storage tanks.* Applied Thermal Engineering, 2005. 25(14): p. 2285-2298.
38. Bouhal, T., et al., *Numerical modeling and optimization of thermal stratification in solar hot water storage tanks for domestic applications: CFD study.* Solar Energy, 2017. 157: p. 441-455.
39. Hahne, E. and Y. Chen, *Numerical study of flow and heat transfer characteristics in hot water stores.* Solar energy, 1998. 64(1-3): p. 9-18.
40. Yaïci, W., et al., *Three-dimensional unsteady CFD simulations of a thermal storage tank performance for optimum design.* 2013. 60(1-2): p. 152-163.
41. Han, Y.M., R.Z. Wang, and Y.J. Dai, *Thermal stratification within the water tank.* Renewable and Sustainable Energy Reviews, 2009. 13(5): p. 1014-1026.
42. Fertahi, S.e.-D.n., A. Jamil, and A. Benbassou, *Review on Solar Thermal Stratified Storage Tanks (STSST): Insight on stratification studies and efficiency indicators.* Solar Energy, 2018. 176: p. 126-145.
43. Chandra, Y.P. and T. Matuska, *Stratification analysis of domestic hot water storage tanks: A comprehensive review.* Energy and Buildings, 2019. 187: p. 110-131.
44. Yang, J., J. Li, and R. Feng, *HEAT LOSS ANALYSIS AND OPTIMIZATION OF HOUSEHOLD SOLAR HEATING SYSTEM.* Heat Transfer Research, 2019. 50(7): p. 659-670.
45. Miller, C. *The effect of a conducting wall on a stratified fluid in a cylinder*. in *12th Thermophysics Conference*. 1977.
46. Armstrong, P., et al., *Improving the energy storage capability of hot water tanks through wall material specification.* Energy, 2014. 78: p. 128-140.
47. Jaluria, Y. and S.K. Gupta, *Decay of thermal stratification in a water body for solar energy storage.* Solar Energy, 1982. 28(2): p. 137-143.

48. Nelson, J.E.B., A.R. Balakrishnan, and S. Srinivasa Murthy, *Parametric studies on thermally stratified chilled water storage systems.* Applied Thermal Engineering, 1999. 19(1): p. 89-115.
49. Fan, J. and S. Furbo, *Buoyancy driven flow in a hot water tank due to standby heat loss.* Solar Energy, 2012. 86(11): p. 3438-3449.
50. Shyu, R.J. and C.K. Hsieh, *Unsteady Natural Convection in Enclosures With Stratified Medium.* Journal of Solar Energy Engineering, 1987. 109(2): p. 127-133.
51. Rodriguez, I., et al., *Unsteady numerical simulation of the cooling process of vertical storage tanks under laminar natural convection.* International Journal of Thermal Sciences, 2009. 48(4): p. 708-721.
52. Holzbecher, M. and A. Steiff, *Laminar and turbulent free convection in vertical cylinders with internal heat generation*. International Journal of Heat and Mass Transfer, 1995. 38(15): p. 2893-2903.
53. Lin, Y. and R. Akins, *Thermal description of pseudosteady-state natural convection inside a vertical cylinder*. International journal of heat and mass transfer, 1986. 29(2): p. 301-307.
54. Kulacki, F.A. and R.J. Goldstein, *Thermal convection in a horizontal fluid layer with uniform volumetric energy sources*. Journal of Fluid Mechanics, 1972. 55(2): p. 271-287.
55. Papanicolaou, E. and V. Belessiotis, *Transient natural convection in a cylindrical enclosure at high Rayleigh numbers*. International Journal of Heat and Mass Transfer, 2002. 45(7): p. 1425-1444.
56. Evans, L., R. Reid, and E.J.A.J. Drake, *Transient natural convection in a vertical cylinder*. 1968. 14(2): p. 251-259.
57. Hyun, J.M., *Transient process of thermally stratifying an initially homogeneous fluid in an enclosure*. International Journal of Heat and Mass Transfer, 1984. 27(10): p. 1936-1938.
58. Lin, W. and S.W. Armfield, *Long-term behavior of cooling fluid in a vertical cylinder*. International Journal of Heat and Mass Transfer, 2005. 48(1): p. 53-66.
59. Lin, W. and S.W. Armfield, *Natural convection cooling of rectangular and cylindrical containers*. International Journal of Heat and Fluid Flow, 2001. 22(1): p. 72-81.
60. Lin, W. and S.W. Armfield, *Direct simulation of natural convection cooling in a vertical circular cylinder*. International Journal of Heat and Mass Transfer, 1999. 42(22): p. 4117-4130.
61. Dinh, T. and R. Nourgaliev, *Turbulence modelling for large volumetrically heated liquid pools.* Nuclear Engineering Design, 1997. 169(1-3): p. 131-150.
62. Lam, C. and K. Bremhorst, A modified form of the k-ε model for predicting wall turbulence. Journal of Fluids Engineering, 1981. 103(3): p. 456-460.
63. Oliveski, R.D.C., A. Krenzinger, and H.A. Vielmo, *Cooling of cylindrical vertical tanks submitted to natural internal convection.* International journal of heat and mass transfer, 2003. 46(11): p. 2015-2026.
64. FLUENT, *FLUENT 6.0 User's Guide*. 2001, Fluent Inc.: 10 Cavendish Court, Lebanon, NH03766, USA.
65. Steinberner, U. and H.-H. Reineke. *Turbulent buoyancy convection heat transfer with internal heat sources*. in *International Heat Transfer Conference Digital Library*. 1978. Begel House Inc.
66. Cengel, Y.A., *Introduction to Thermodynamics and Heat transfer* M. Hackett, Editor. 2008, McGraw-Hill: New York, America.
67. Fishbaugher, M.J., *Natural convection and conduction in a vertical annulus with a concentric baffle: a numerical study.* 1988.

68. Pushpa, B., M. Sankar, and O.D. Makinde, *Optimization of thermosolutal convection in vertical porous annulus with a circular baffle.* Thermal Science Engineering Progress, 2020. 20: p. 100735.